31 Jul 89 Conference Presentation

Unsteady Flows Produced by Small Amplitude Oscillations of the Canard of an X-29 Model

TA 2307-F1-38

T. Mouch, T. McLaughlin, J. Ashworth

F.J. Seiler Research Laboratory
USAF Academy CO 80840-6528

FJSRL-PR-90-0017

Distribution Unlimited

This investigation develops previous flow visualization studies by quantifying the flowfield around the tandem wing of an X-29 model in the wake of an oscillating canard. The local velocity above and below the wing was measured with the canard oscillating and compared to the cases with the canard static. A structured disturbance pattern was documented in the wake of the oscillating canard then compared to the random flow pattern behind the static canard. Considering the dual vortex system shed from the oscillating canard, the tip vortex dominates the flowfield. The leading edge vortex passes well above the wing.

flow visualization
three dimensional flow
hot wire anemometers

10

UNCLASSIFIED UNCLASSIFIED UNCLASSIFIED NONE

UNSTEADY FLOWS PRODUCED BY SMALL AMPLITUDE OSCILLATIONS OF THE CANARD OF AN X-29 MODEL

T. Mouch*, T. McLaughlin** and J. Ashworth***
HQ USAFA/DFAN
U.S. Air Force Academy
Colorado Springs, CO 80840-5701

Abstract

This investigation develops previous flow visualization studies[7,10,14] by quantifying the flowfield around the tandem wing of an X-29 model in the wake of an oscillating canard. The local velocity above and below the wing was measured with the canard oscillating and compared to the cases with the canard static. A structured disturbance pattern was documented in the wake of the oscillating canard then compared to the random flow pattern behind the static canard. Considering the dual vortex system shed from the oscillating canard, the tip vortex dominates the flowfield, the leading edge vortex passes well above the wing.

*Major, USAF
Assistant Professor, Dept of Aeronautics,
Senior Member AIAA

**Captain, USAF
Instructor, Dept of Aeronautics
Member ISA

***Lieutenant Colonel, USAF
Associate Professor, Dept of Aeronautics
Member AIAA

Nomenclature

AOA	Model Angle of Attack (referenced to the freestream velocity)
c	Canard chordlength measured at midspan (c = 6 inches)
V_∞	Freestream tunnel velocity
K	Nondimensional reduced frequency parameter, $K = \frac{\omega c}{2V_\infty}$
ω	Rotational frequency (in radians per second)
α	Canard angle of attack (referenced to model centerline)
α_m	Mean angle of attack for canard
α_ω	Oscillation amplitude of canard about α_m
Φ	Nondimensional oscillation cycle (percent of the cycle beginning at α_{max})

Introduction

Numerous studies on forced unsteady oscillations, both experimental and theoretical, have demonstrated lift enhancements derived from the effective control of these flows.[1-9,10,16] To demonstrate the practical application of these flows, an investigation comparing flow visualization and hotwire velocity measurements about an X-29 model was conducted. The canard is driven through small amplitude oscillations about the midchord line. Previous investigations have demonstrated the practical application of large amplitude oscillations of the canard.[14] The current investigation concentrates on the use of small amplitude oscillations which are feasible in direct application to advanced aircraft. The small amplitude unsteady flow visualization data show flow attachment to the canard, similar to larger amplitude oscillations, at angles of attack well above static canard stall. Furthermore, the canard tip and leading edge vortices produce a cyclic effect on the tandem forward-swept wing. Hotwire velocity measurements were taken above and below the wing, at conditions identical to the flow visualization data. These velocity fluctuations illustrate the enhanced velocity fields about the tandem wing caused by the dynamic motion of the canard. These velocity measurements quantify the flow field about the tandem wing and support hypotheses developed from the flow visualization. Thus, the dynamic motion of the canard at smaller amplitudes produces effects similar to the larger amplitudes while preventing excessively heavy stresses on the control surface.

Methods

A 1/10-scale, reflection-plane model of the X-29 aircraft (Fig. 1) was installed on the floor of the U.S. Air Force Academy 3 x 3 ft. subsonic wind tunnel. The canard was attached to a "Scotch-yoke" oscillation mechanism which was driven by a variable speed motor (Fig. 2). Minimum and maximum canard angles were set and the tunnel was operated at 25 ft/sec. The motor drove the canard at an oscillation frequency of approximately 16 Hz which gives a K-value of one. A reed switch on the oscillation mechanism produced trigger pulses each time the canard reached maximum α. The nondimensional oscillation phase angle, Φ is equal to 0.0 when the canard was at the maximum angle of attack and equal to 1.0, 2.0 etc. when the canard has passed through one cycle and returned to α_{max}. After applying signal conditioning to this trigger pulse to produce a sharp transition, the signal triggered a computer controlled data acquisition system (DAS).

A hot wire positioned in the flow measured local velocity variations. Upon canard trigger, the DAS accepted hot wire anemometry data for four complete canard cycles, at a rate of 256 samples per oscillation period. This process was repeated 50 times, each time triggering at the same point in the canard cycle. Hot wire data from the 50 repetitions were ensemble averaged by the DAS to filter system noise, leaving only the repetitious variation in flow speed as an output signal. The local velocity is nondimensionalized to the freestream velocity. Dynamic (canard oscillating with $\alpha_m = 12^\circ$ and $\alpha_w = 5^\circ$) data was referenced to data collected with the canard static at $\alpha = 7$, 12 and 17 degrees. The entire process was repeated with the hot wire 2 inches above, 1 inch above and 1 inch below the tandem wing at 1/10 chord increments starting at the leading edge. Two vertical planes, identical

to the flow visualization experiments of Ref. 14, were investigated downstream of the canard tip and midspan.(Fig 1).

Results

Figure 3 provides a visualization of the flow phenomena occurring in the vicinity of the oscillating canard and tandem wing of the X-29 model. This photograph was taken with $\Phi=0.3^{14}$ and shows a twin vortex system shed by the oscillating canard. The first vortex, which is shed from the leading edge can be seen passing above the tandem wing just forward of the trailing edge This vortex appears to have little or no effect on the flowfield about the tandem wing. The second vortex is shed from the canard tip and can be seen impinging on the leading edge of the tandem wing. This vortex seems more dominant in the flow field about the tandem wing. From the flow visualizations, this unsteady flowfield is shown to be orderly and repeatable. The temporal and spatial relationship between these vortices show in the visualizations aid in understanding the velocity fluctuations recorded by the hotwire probe.

Figures 4a and 5a show two-dimensional plots of nondimensional velocity vs. phase cycle, with Φ= 0.0 on the left. Dashed lines in these figures represent the standard deviation of the local velocity for the canard static case. Figs. 4b and 5b are three-dimensional plots of chord position vs. phase cycle with nondimensional velocity in the vertical. Note: the leading edge of the wing is in the upper left of the graph and Φ= 0 is on the far right.

Hotwire at Midspan

Fig. 4a shows hotwire velocity traces in a vertical plane with the canard midspan and 2 inches above the tandem wing. Small velocity fluctuations can be seen at the leading edge and midchord stations, however these dissipate by the trailing edge. The velocity with the canard oscillating is nearly equal to the static case. In Fig. 5a, the velocity fluctuations cause "ridges" which identify high velocity regions and convection of these peaks along the chord. These ridges also dissipate before reaching the trailing edge.

Along the 1 inch plane above the wing, the leading edge station shows a more cohesive flow pattern with higher velocity fluctuations. Tracing the structure from the leading to the trailing edge, a phase shift in the velocity peak denotes convection of the upper surface disturbance. This shift is especially noticeable as a shift in the ridge shown in Fig. 5a for 1 inch above the wing.

Completing the study of flow behind the midspan of the canard in Fig. 4a, observations at 1 inch below the wing show an even stronger velocity flow pattern defining the flowfield. The repeatability is very noticeable as well as the phase shift. Velocity magnitudes in this region are generally below freestream values, indicating higher pressures and a distinct drop in local velocity between the leading edge and the midchord station. The canard static data show the influence of canard stall on the local velocity of the tandem wing. With α= 7°, the canard hasn't stalled and the local velocity is near freestream, while at 12° and 17°, the local velocity is below freestream due to the wake behind the stalled canard.

Hotwire at Tip

Starting at 2 inches above the tandem wing (Fig. 4b), the distinct repeatability of the flow field is

observed over the tandem wing in plane with the canard tip. Ensemble averaging left a very orderly trace. This orderly trace is evidenced by the thin clean line for the time-dependent velocity, especially at the trailing edge.

At 1 inch above the wing, the cyclic nature of the flowfield is evident. Notice also the large flux in velocity, suggesting the strong effect of the canard tip vortex seen in Fig 3. A phase shift in peak velocities as this orderly flowfield traverses the wing is evident both in Fig. 4b and 5b. Comparing the leading edge and midchord positions, notice the large change in velocity magnitude.

Concluding these results at 1 inch below the wing, very little effect of any vortical structure and a fair amount of randomness in the local velocity were seen even with the canard oscillating. Fig 5b shows minimal structure and a very low "ridge"

The data shown in Figs. 4 and 5 also contain static local velocity information. Due to the randomness of flow behind a stalled surface, this velocity data is given as the mean of the measured velocity (solid line) and one standard deviation (dashed lines). Through a comparison of the velocities behind the static canard, the approximate stall angle can be determined. Thus with the canard at $\alpha = 7^\circ$, the flow is still attached due to the higher measured velocity. While with the canard at α's of 12° and 17°, lower velocities were measured due to the region of separated flow behind the stalled canard. It is in this region of α's that an oscillating canard can be used to an advantage.

Discussion

The data shown in Figs. 4 and 5 was taken with a single hotwire and thus gives velocity magnitudes only. Direction can not be inferred directly from the velocity data. To determine direction, further study would be necessary with an X-wire hotwire. But, at the present time, comparing these velocity measurements with the flow visualization of Fig. 3 will help indicate relative direction.

Thus comparing Fig. 3 to the velocity measured at the tip (Fig. 4b and 5b), a strong effect of the tip vortex shed by the oscillating canard is shown. A well-defined structure evidenced by the repeatable flow pattern and large velocity magnitude variations is due to the passage of the tip vortex (as seen in Fig. 3). These large velocity fluctuations could produce cyclic structural loading and the effects of these should be studied further.

The counterclockwise flow of the tip vortex, (as viewed downstream from the nose of the model), impinging on the leading edge of the wing in Fig. 3 would cause a large increase in the local α and could lead to local flow separation on the wing. Local separation could explain the large drop of the overall velocity profile measured at the hotwire position behind the canard-tip at the midchord and trailing edge positions shown in Figs. 4b and 5b.

When considering the flow pattern at the canard midspan, the "crank" in the wing will also have an effect. The large velocity fluctuations on the underside of the midspan could be due to formation of a vortex due to the cyclic downwash change about the crank. Thus, the crank could cause a velocity fluctuation due to streamwise vorticity and warrants further investigation. This effect was visualized in ref. 18.

Conclusions

From previous investigations, large amplitude oscillations of the canard provide a positive effect on the flow field about both the canard and the tandem wing. But these large amplitudes may not have a practical aircraft application. Thus the possibility of small amplitude oscillations were investigated. Data from this investigation shows a similar benefit at a more practical condition. The flow visualization (Fig. 3) shows the canard tip vortex has a greater effect on the flow over the tandem wing than the leading edge vortex. The quantitative data confirms the largest velocity fluctuations are behind the canard tip. Thus, the tip vortex and not the leading edge vortex dominates tne flowfield in the vicinity of the tandem wing.

From previous studies, one can see the positive effect of oscillating a canard as the flow will stay attached past the static stall α. This study has shown some effects of oscillating a canard on the flow field near the tandem wing. But the data from this study does not provide conclusive evidence as to a positive effect on the tandem wing due to the canard's oscillation and warrants further study.

Finally, the effects of the cyclic loading of the tandem wing due to the flow field induced by the oscillating canard could have some structural consequences and also deserves further study.

Acknowledgements

The authors would like to thank Maj Vincent Parisi and Mr Larry Schaible for their valuable assistance in this effort. Without their help, this investigation would not have been successfully completed.

References

1. McCroskey, W.J., " Unsteady Airfoils," Annual Review of Fluid Mechanics, 1982, pp. 285-311.

2. Robinson, M.C. and Luttges, M.W., "Unsteady Flow Separation and Attachment Induced by Pitching Airfoils," AIAA-83-0131, AIAA 21st Aerospace Sciences Meeting, Reno, NV, Jan. 1983.

3. Reynolds, W.C. and Carr, L.W., "Review of Unsteady, Driven, Separated Flows," AIAA Shear Flow Control Conference, Boulder, CO, March 1985.

4. Adler, J.N. and Luttges, M.W., "Three-dimensionality in Unsteady Flow About a Wing," AIAA-85-0132, AIAA 23rd Aerospace Sciences Meeting, Reno, NV, Jan. 1985.

5. Ashworth, J. and Luttges, M.,"Comparisons in Three-dimensionality in the Unsteady Flows Elicited by Straight and Swept Wings," AIAA-86-2280CP, AIAA Atmospheric Flight Mechanics Conference, Williamsburg, VA, August 1986.

6. Ashworth, J., Waltrip, M. and Luttges, M., "Three-Dimensional Unsteady Flow Fields Elicited by a Pitching Forward Swept Wing," AIAA-86-1104, AIAA 4th Joint Fluid Mechanics, Plasma Dynamics and Lasers Conference, Atlanta, GA, May 1986.

7. Ashworth, J., Huyer, S. and Luttges, M., "Comparisons of Unsteady Flow Fields about Straight and Swept Wings Using Flow Visualizations and Hotwire Anemometry," AIAA-87-1334, AIAA 19th Fluid Dynamics, Plasma Dynamics and Lasers Conference, Honolulu, Hawaii, June 1987.

8. Freymuth, P., Finnaish, F. and Bank, W., "Visualization of Wing Tip Vortices in Accelerating and Steady Flow," Journal of Aircraft, Vol. 23, No. 9, Sept. 1986, pp.730-733.

9. Gad-el-Hak, M. and Ho. C., "Unsteady Vortical Flow Around Three-Dimensional Lifting Surfaces," AIAA Journal, Vol. 24, No. 5, pp. 713-721, May 1986.

10. Ashworth, J., Mouch, T. and Luttges, M., " Application of Forced Unsteady Aerodynamics to a Forward Swept Wing X-29 Model,"AIAA-88-0563, AIAA 26th Aerospace Sciences Meeting, Reno, NV, Jan. 1988.

11. Moore, M. and Frei, D., "X-29 and Forward Swept Wing Aerodynamic Overviews," AIAA-83-1834, AIAA Applied Aerodynamics Conference, Danvers, MA, July 1983.

12. Robinson, M.C., Helin, H.E. and Luttges M.W., "Control of Wake Structure Behind an Oscillating Airfoil," AIAA-86-2282-CP, AIAA Atmospheric Flight Mechanics Conference, Williamsburg, VA, August 1986.

13. Schlichting, H., Boundary Layer Theory, McGraw-Hill Co., Sixth Edition, 1968.

14. Ashworth, J., Mouch, T. and Luttges, M., "Visualization and Anemometry Analyses of Forced Unsteady Flows about an X-29 Model," AIAA-88-2570, AIAA 6th Applied Aerodynamics Conference, Williamsburg, VA, June 1988.

15. Robinson, M. and Wissler, J., "Pitch Rate and Reynolds Number Effects on a Pitching Rectangular Wing," AIAA-88-2577, AIAA 6th Applied Aerodynamics Conference, Williamsburg, VA, 1988.

16. Huyer, S., and Luttges, M., "Unsteady Flow Interactions Between the Wake of an Oscillating Airfoil and a Stationary Trailing Airfoil," AIAA-88-2581, AIAA 6th Applied Aerodynamics Conference, Williamsburg, VA, 1988.

17. Walker, J. and Robinson, M., "Impingement of Orthogonal Unsteady Vortex Structures on Trailing Aerodynamic Surfaces," AIAA-88-2580, AIAA 6th Applied Aerodynamics Conference, Williamsburg, VA, 1988.

18. Ashworth, J, Three-Dimensional Unsteady Flow Elicited By Finite Wings and Complex Configurations, PhD Dissertation, Dept of Aerospace Engineering Sciences, University of Colorado, Boulder, CO, 1987, Ch VII-VIII

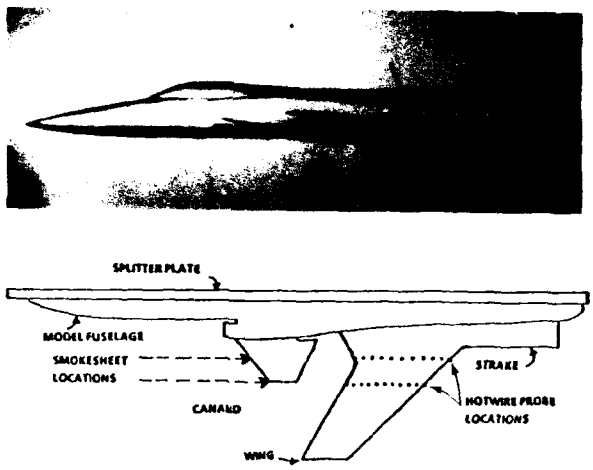

Fig 1. X29 Schematic and Hotwire Probe Locations

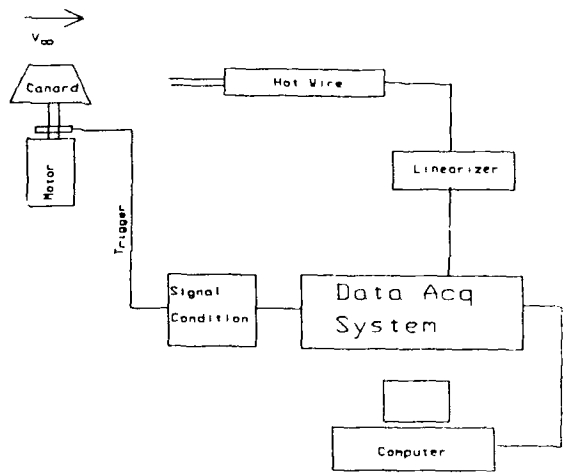

Fig 2. Data Acquisition Set-up

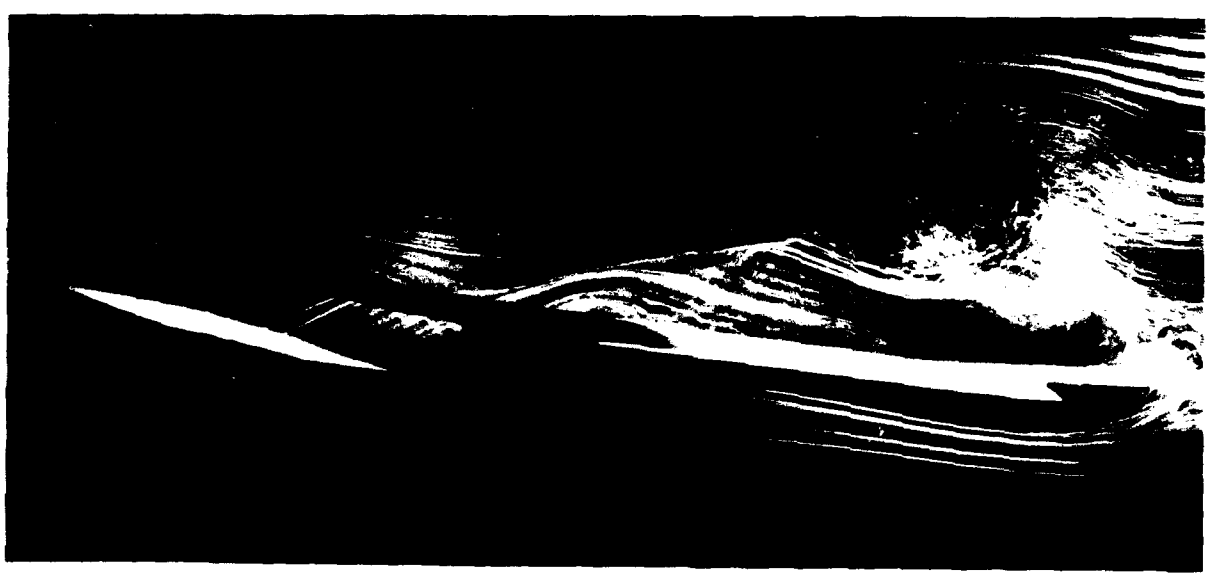

Fig 3. Flow Visualization Photo, Canard $\Phi \approx 0.3$

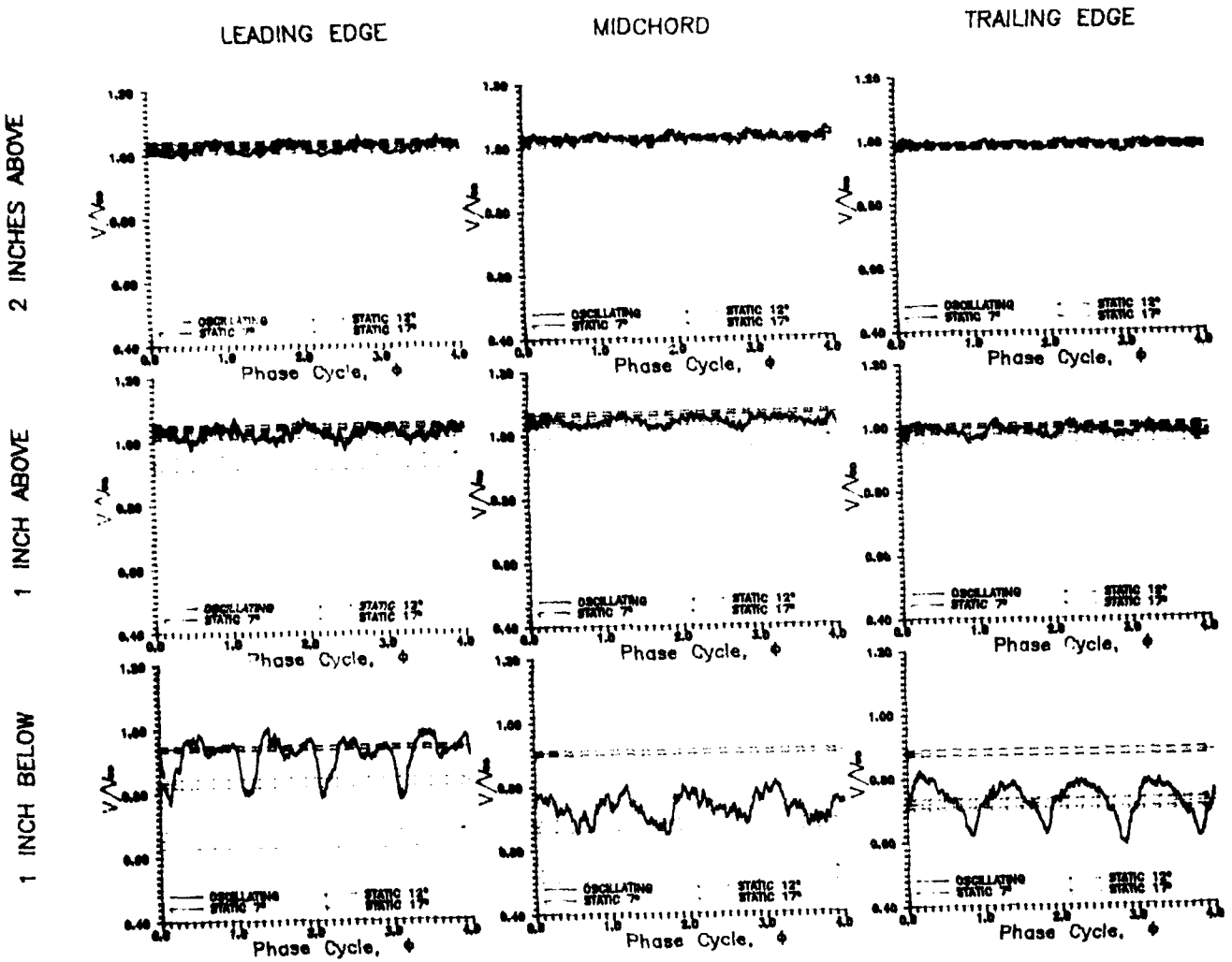

Fig 4a. Hotwire Velocity Traces - Behind Midspan of the Canard

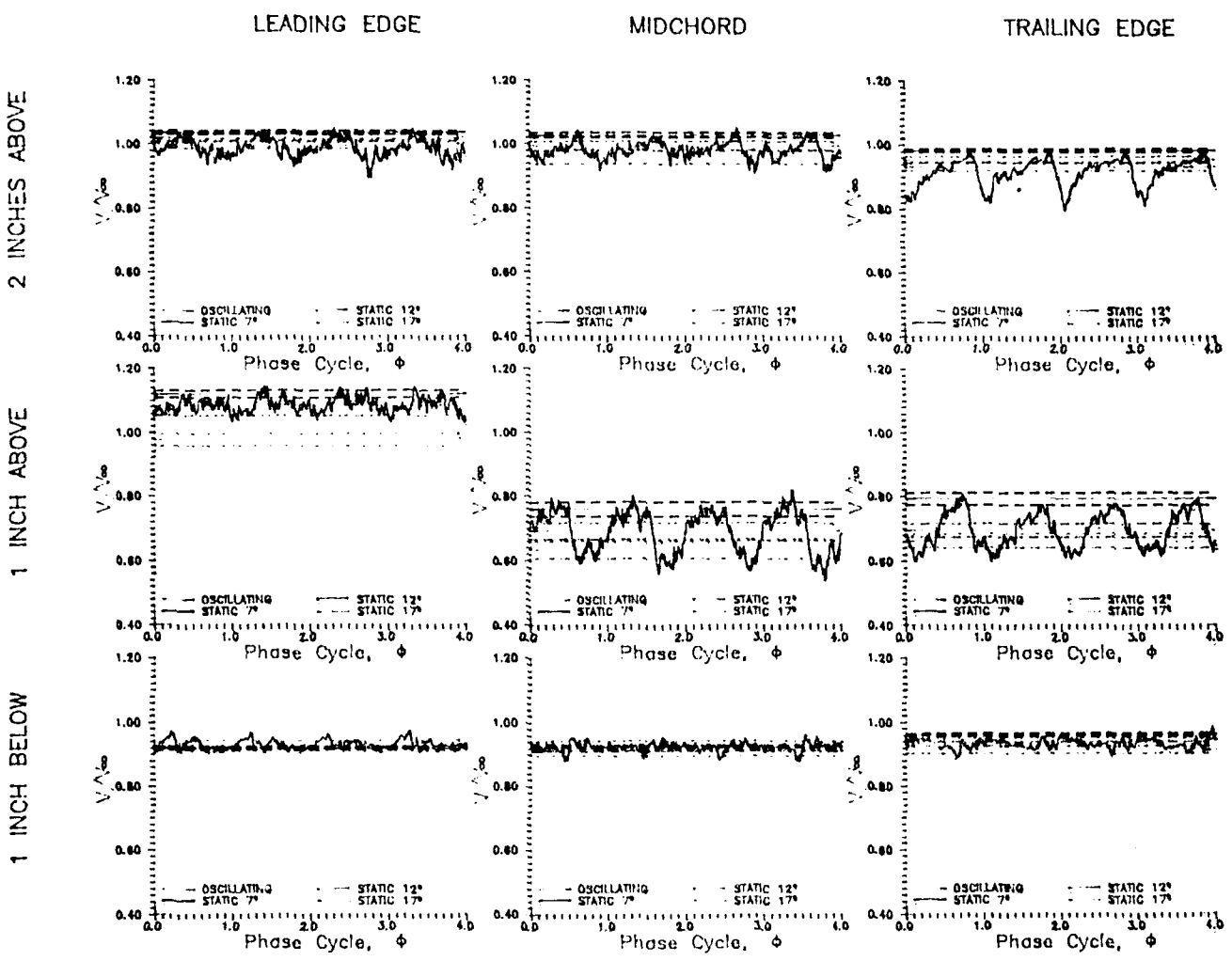

Fig 4b, Hotwire Velocity Traces - Behind Tip of the Canard

Fig 5. Three Dimensional Velocity Plots,
a - Behind Midspan of the Canard, b - Behind Tip of the Canard